Science Advances
AAAS

Supplementary Materials for

Distributed interfacing by nanoscale photodiodes enables single-neuron light activation and sensory enhancement in 3D spinal explants

Agnes Thalhammer *et al.*

Corresponding author: Laura Ballerini, ballerin@sissa.it

Agnes Thalhammer, athalham@sissa.it

Sci. Adv. **8**, eabp9257 (2022)
DOI: 10.1126/sciadv.abp9257

The PDF file includes:

Other Supplementary Material for this manuscript includes the following:

SUPPLEMENTARY MATERIAL

Supplementary Video V1 | Network activity in the dorsal spinal cord. Neurons are labelled with GCaMP7f (fluorescent levels of calcium transients here displayed as false colors). The video represents the increase in dorsal horn network activity as response to a laser stimulation directed onto single nPD-contacting excitatory neuron. A white dot in the top left corner appears to indicate the timing of stimulation.

Supplementary Video V2 | GABAergic neurons in the dorsal spinal cord were identified via tDTomato labelling, and calcium imaging was performed exploiting GCaMP7f (fluorescent levels here displayed as false colors). The video represents the decrease in network activity in

response to laser stimulation directed onto single nPD-contacting inhibitory, GABAergic neuron. A white dot in the top left corner appears to indicate the stimulation time. **Supplementary Video V3 |** Network activity in the ventral spinal cord. Neurons are labelled with GCaMP7f (fluorescent levels here displayed as false colors). The video represents the increase in synchronization of rhythmic neuronal activity in response to laser stimulation directed onto single nPD-interfaced excitatory neuron. A white dot appears in the top left corner, to indicate the timing of stimulation.

Supplementary figures

Figure S1 | Optical property of the nanocrystalline silicon. Note that the graph confirms at 300K the efficient optical absorption of nPD at the near-infrared (NIR) region. Adapted from[50].

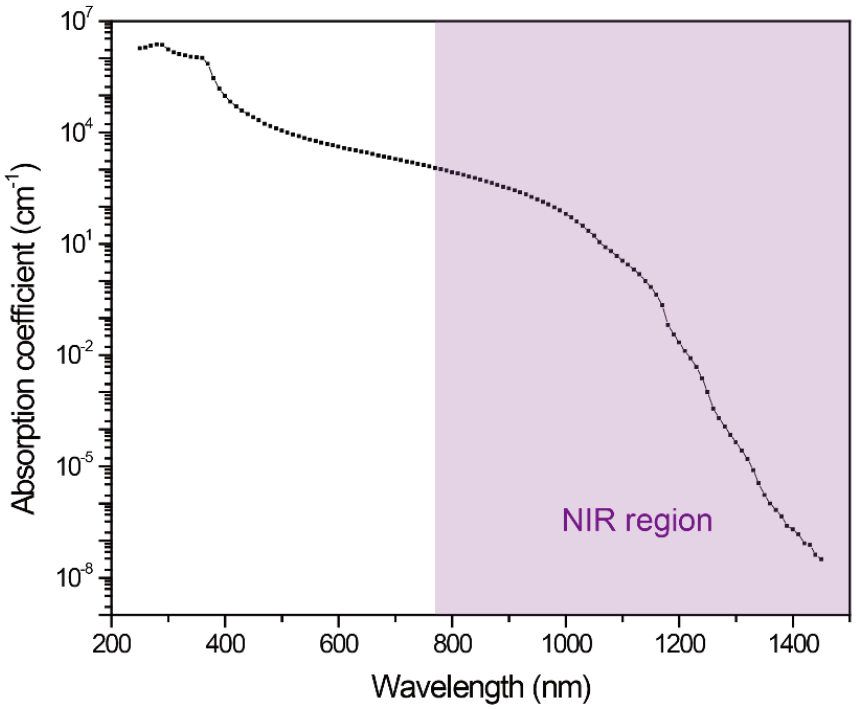

Figure S2 | **Confocal microscopy to selectively photostimulate identified neurons retaining nPD (a)** Brightfield image of SiNWs (nPDs, arrows) on OSC. ROIs for laser stimulation is highlighted in purple. **(b)** Fluorescence image highlights cells filled with Ca^{2+} indicator Fluo-4. The red ROI was selected from the cell with nPD for laser stimulation, but excluding the site of focused stimulation, blue and light blue ROIs depict neighboring neurons. **(c)**Fluorescence transients recorded from ROIs in (b) in response to a 125 ms stimulation with a 20 mW UV laser at 405 nm. Traces are matched in color and numbers with ROIs in (b). In the cell directly stimulated by nPDs a robust calcium response can be observed. **(d)** Bright field image (left) of a hippocampal culture neuron with nPDs placed at variable distance from the cell soma, the red circle highlights the spot of laser illumination, with the nPD at <8 μm from the sample cell (dashed black circle) and the inset shows the fluorescence tracing of the same neuron. Note the absence of response at the time of stimulation (indicated by red shaded area). Box plots summarize peak frequency (middle) and average amplitude (right) before and after stimulation of the nPDs close to the recorded cells but not in direct contact with the cell body (as imaged on the left) do not change. N=12 cultures, paired Student's t-test.

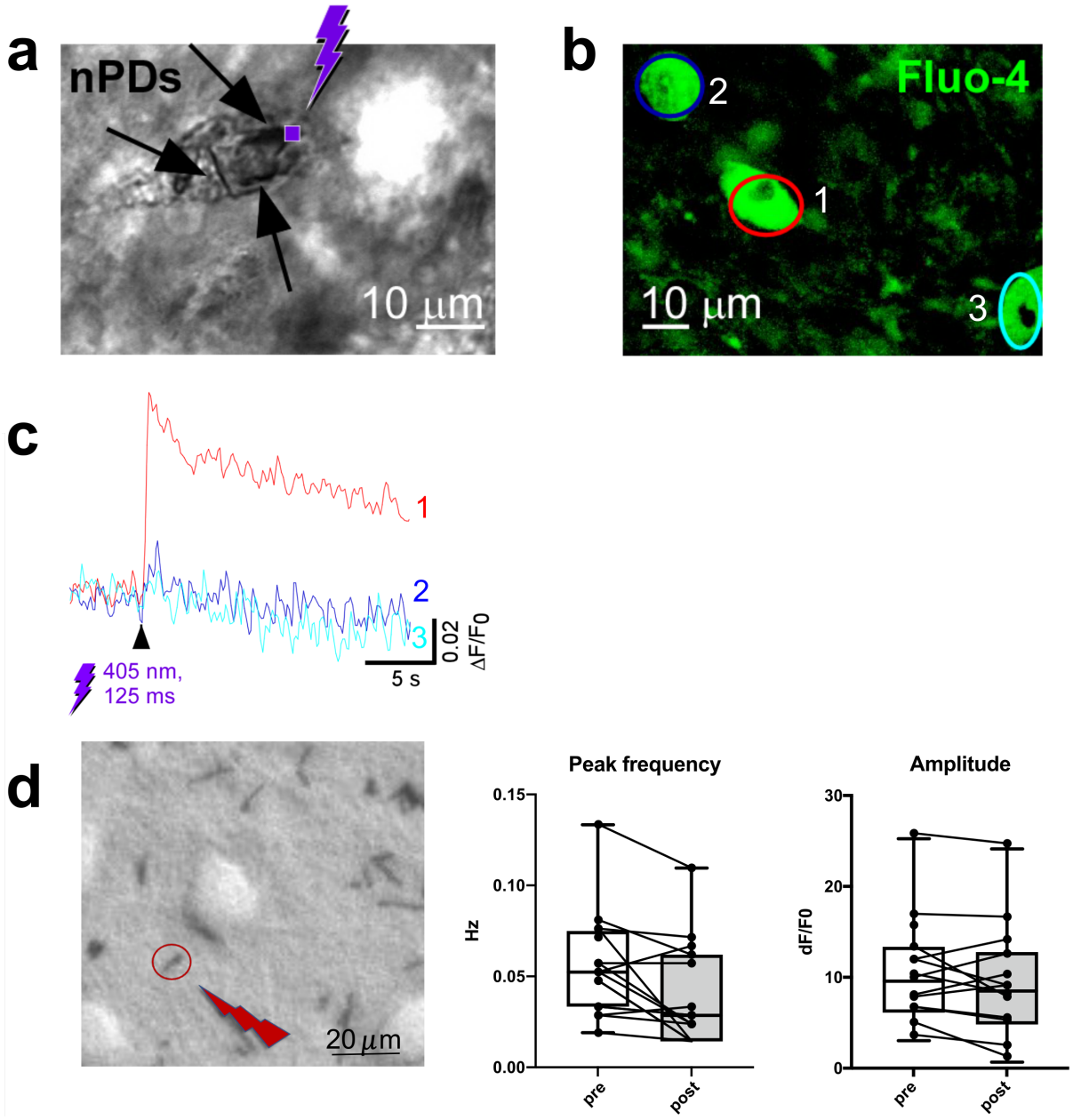
a
nPDs
10 µm
b
Fluo-4
2
1
10 µm
3
c
1
2
3
405 nm,
125 ms
0.02
ΔF/F0
5 s
d
20 µm
Peak frequency
Hz
0.15
0.10
0.05
0.00
pre
post
Amplitude
dF/F0
30
20
10
0
pre
post

Figure S3 | Multiunit activity evoked by light activation of nPD and calcium imaging of action potential dependent neuronal activity (a) Extracellular recordings from VH in OSC incubated with nPDs during NIR light stimulations (20 mW, 40 ms ON - 40 ms OFF, red flash) of a single visually identified nPD neuron. Bottom: magnified evoked multiunits burst (note the different time scale). **(b)** Calcium transients observed in slices expressing GCaMP7f (black) under control of a Syn1 promotor are abolished in the presence of 1 μm TTX (blu), confirming their neuronal origin. **(c)** Dose-repsonse (D/R) curve for laser-mediated stimulation. The change in frequency of GCaMP7f transients in DH neurons is expressed as percentual increase (after the stimulation) over the baseline. Each dot represents a specific laser intensity used for stimulation and the arrow indicate the most used intensity. Data were fitted with a Sigmoid function (see Methods); n=16 slices. **(d)** Inset, bright field image of sample stimulated cell with nPD; fluorescent tracings recorded from NIR light nPDs stimulated cells (black: DH neuron; green: GABAergic neuron; time point (and lengths) of stimulation is indicated by the red shaded area). **(e)** Peak frequency (left) and amplitude (right) before and after laser stimulation of DH neurons by undoped SiNWs (incapable of charge separation upon light stimulation) do not change; n=9 slices, paired Student's t-test. Inset on right top: Bright field image of stimulated cell showing the undoped SiNW and in the corresponding calcium fluorescent tracings the time point (and length) of stimulation is indicated (red shaded area).

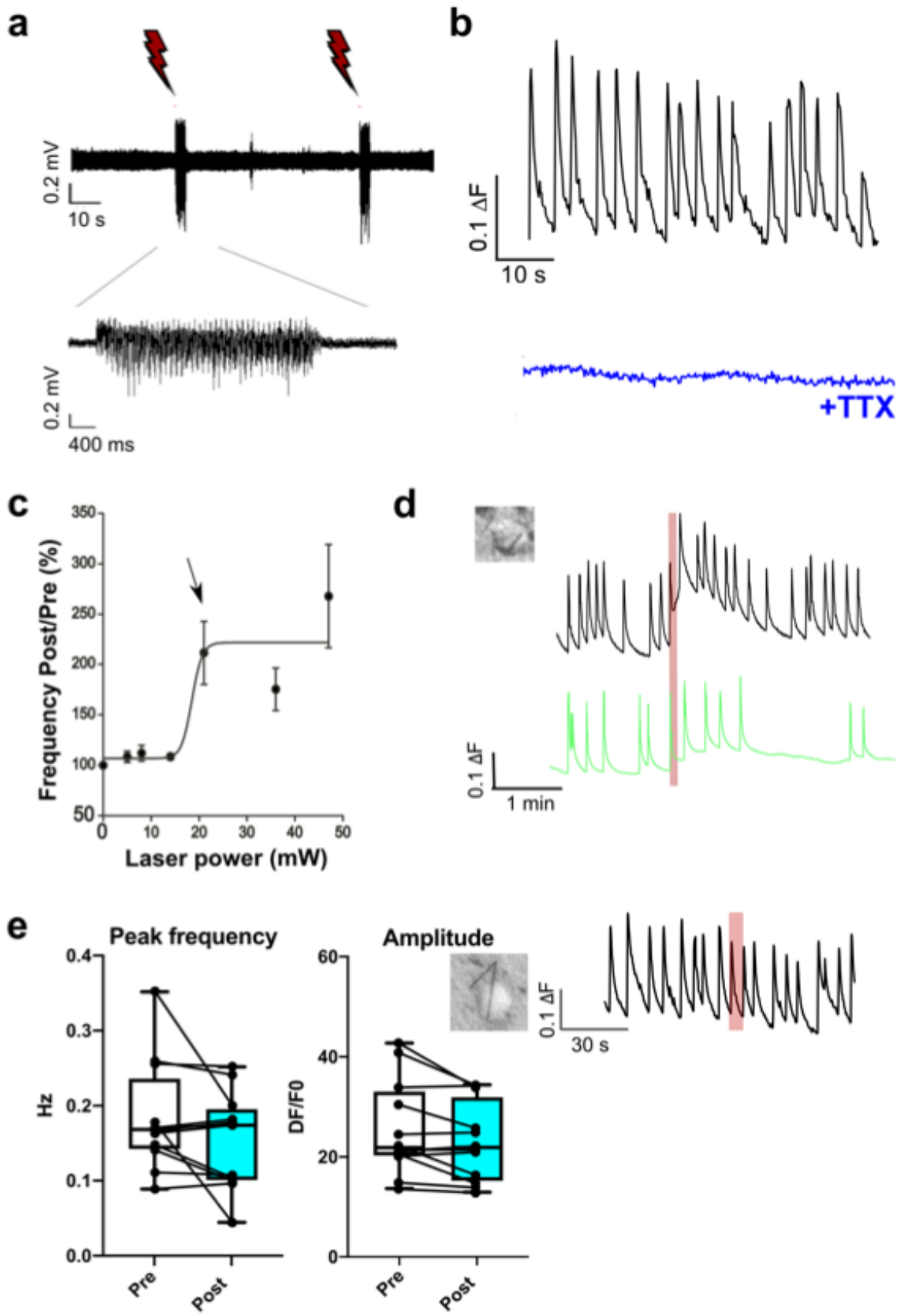
a
0.2 mV
10 s
0.2 mV
400 ms
b
0.1 ΔF
10 s
+TTX
c
Frequency Post/Pre (%)
Laser power (mW)
d
0.1 ΔF
1 min
e
Peak frequency
Hz
Pre
Post
Amplitude
DF/F0
Pre
Post
0.1 ΔF
30 s

Figure S4 | GABAergic neurons in DH spinal cultures (a) Confocal images of OSC DH stained for NeuN (cyan) and GABA (red). **(b)** Box plot quantifies the proportion of GABAergic neurons, n=3 slices.

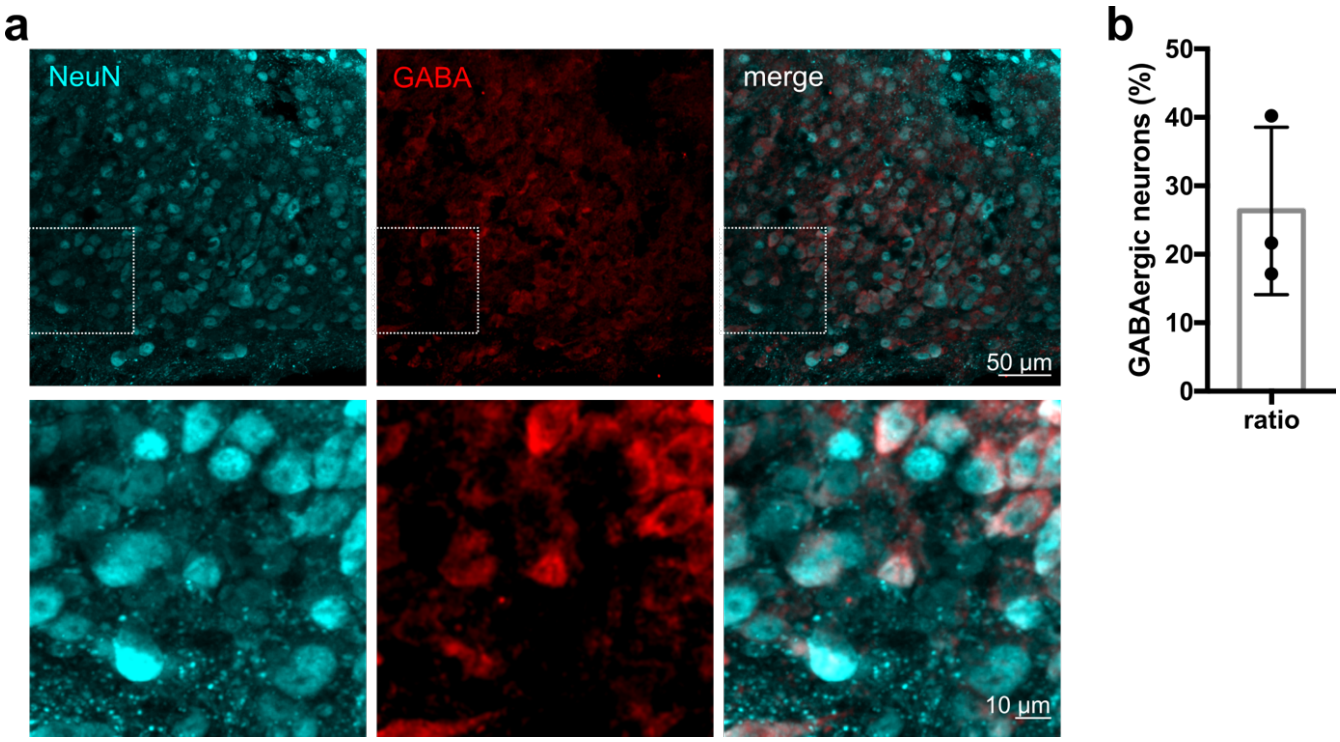

Figure S5 | Functionalization of SiNWs SiNWs were modified using silane anchoring linkers (APTES, blue) and adding maleimide functional group (red). Further attachment of the antibody was achieved by Michael addition of thiolated antibody stem to maleimide functional group. Antibody functionalization was validated using confocal microcopy after binding of fluorescent secondary antibody and using electrochemical impedance measurements.

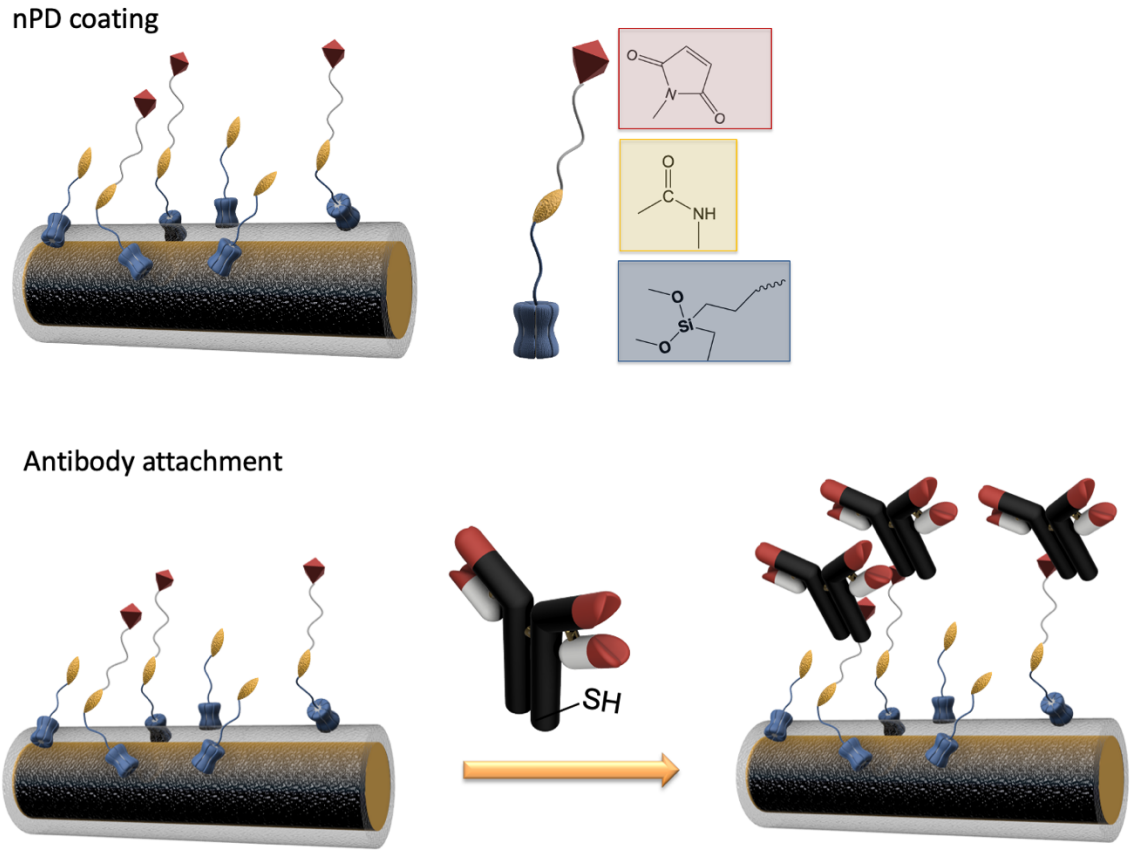

Figure S6 | 24-hour OSC incubation with nPDs (a) Superresolution microscope images (original stack on top left) and 3D reconstruction of small area (top right) of OSC incubated with nPDs (in blue) for 24 hrs. Cell membranes are highlighted in green (ConA-staining), cell nuclei in pink and lysosomes in red. nPDs appear to be stably integrated to the slice tissue with variable orientations. **(b)** GCamP7f traces recorded from the stimulated cells upon 24 hrs of saline (black) and nPDs (green, left bright field image of the cell with nPDs) incubation. Timepoint of laser stimulation is highlighted by red bar and flash. Note the transient increase in baseline fluorescence during stimulation when in the presence of 24 hrs old nPD **(c)** Quantification of baseline calcium events' frequency, prior to stimulation, which is not affected by 24 hrs of nPD incubation (n=8 slices). **(d)** Increase in calcium events' frequency by laser stimulation of nPDs in the DH is preserved also after 24 hrs of nPDs incubation (n=8 slices, $p<0{,}001$, unpaired Student's t-test with Welch correction). **(e, f)** GFAP (in green) and Iba1 (in red) confocal images of OSC slices upon saline and 24 hrs nPDs incubations. Resident cells (astrocytes and microglia) reactivity was not triggered by nPDs, quantified in (f). Calibration bar 50 µm; n=12 slices.

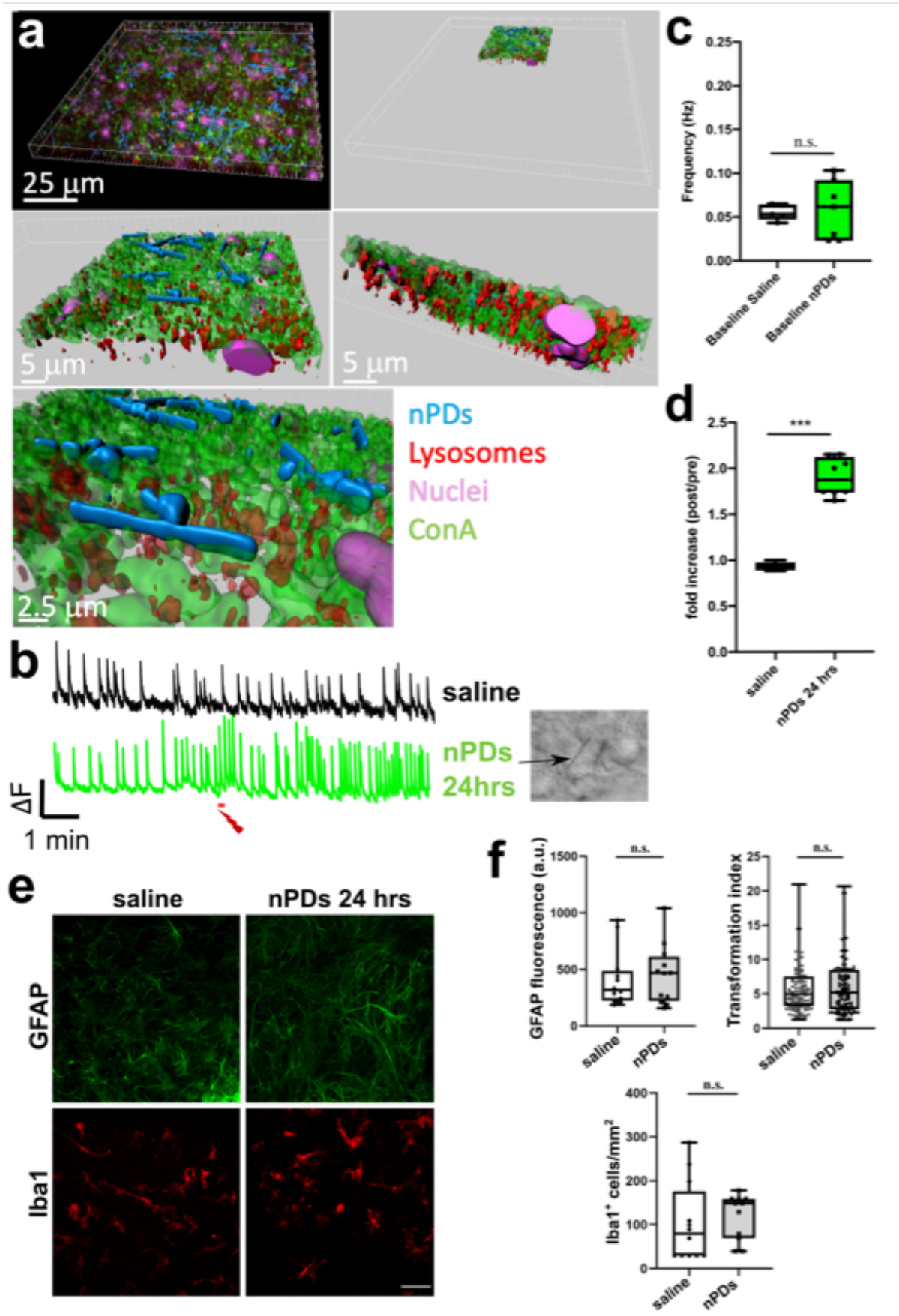
a
25 µm
5 µm
5 µm
2.5 µm
nPDs
Lysosomes
Nuclei
ConA
c
Frequency (Hz)
n.s.
Baseline Saline
Baseline nPDs
d
fold increase (post/pre)
***
saline
nPDs 24 hrs
b
saline
nPDs
24hrs
ΔF
1 min
e
saline
nPDs 24 hrs
GFAP
Iba1
f
GFAP fluorescence (a.u.)
n.s.
saline
nPDs
Transformation index
n.s.
saline
nPDs
Iba1+ cells/mm2
n.s.
saline
nPDs

REFERENCES AND NOTES

1. J. S. Perlmutter, J. W. Mink, Deep brain stimulation. *Annu. Rev. Neurosci.* **29**, 22–257 (2006).

2. K. Ashkan, P. Rogers, H. Bergman, I. Ughratdar, Insights into the mechanisms of deep brain stimulation. *Nat. Rev. Neurol.* **13**, 548–554 (2017).

3. P. Gupta, N. Balasubramaniam, H.-Y. Chang, F.-G. Tseng, T. S. Santra, A single-neuron: Current trends and future prospects. *Cell* **9**, 1528 (2020).

4. M. C. Romero, M. Davare, M. Armendariz, P. Janssen, Neural effects of transcranial magnetic stimulation at the single-cell level. *Nat. Commun.* **10**, 2642 (2019).

5. M. Diamantaki, S. Coletta, K. Nasr, R. Zeraati, S. Laturnus, P. Berens, P. Preston-Ferrer, A. Burgalossi, Manipulating hippocampal place cell activity by single-cell stimulation in freely moving mice. *Cell Rep.* **23**, 32–38 (2018).

6. B. Knauer, M. C. Stüttgen, Assessing the impact of single-cell stimulation on local networks in rat barrel cortex—A feasibility study. *Int. J. Mol. Sci.* **20**, 2604 (2019).

7. G. Doron, M. Brecht, What single-cell stimulation has told us about neural coding. *Philos. Trans. R. Soc. B Biol. Sci.* **370**, 20140204 (2015).

8. R. Parameswaran, J. L. Carvalho-de-Souza, Y. Jiang, M. J. Burke, J. F. Zimmerman, K. Koehler, A. W. Phillips, J. Yi, E. J. Adams, F. Bezanilla, B. Tian, Photoelectrochemical modulation of neuronal activity with free-standing coaxial silicon nanowires. *Nat. Nanotechnol.* **13**, 260–266 (2018).

9. J. Rivnay, H. Wang, L. Fenno, K. Deisseroth, G. G. Malliaras, Next-generation probes, particles, and proteins for neural interfacing. *Sci. Adv.* **3**, e1601649 (2017).

10. D. Avossa, M. Grandolfo, F. Mazzarol, M. Zatta, L. Ballerini, Early signs of motoneuron vulnerability in a disease model system: Characterization of transverse slice cultures of spinal cord isolated from embryonic ALS mice. *Neuroscience* **138**, 1179–1194 (2006).

11. S. Usmani, E. R. Aurand, M. Medelin, A. Fabbro, D. Scaini, J. Laishram, F. B. Rosselli, A. Ansuini, D. Zoccolan, M. Scarselli, M. De Crescenzi, S. Bosi, M. Prato, L. Ballerini, 3D meshes of carbon nanotubes guide functional reconnection of segregated spinal explants. *Sci. Adv.* **2**, e1600087 (2016).

12. V. Giacco, G. Panattoni, M. Medelin, E. Bonechi, A. Aldinucci, C. Ballerini, L. Ballerini, Cytokine inflammatory threat, but not LPS one, shortens GABAergic synaptic currents in the mouse spinal cord organotypic cultures. *J. Neuroinflammation* **16**, 127 (2019).

13. A. I. Basbaum, D. M. Bautista, G. Scherrer, D. Julius, Cellular and molecular mechanisms of pain. *Cell* **139**, 267–284 (2009).

14. S. C. Koch, D. Acton, M. Goulding, Spinal circuits for touch, pain, and itch. *Annu. Rev. Physiol.* **80**, 189–217 (2018).

15. B. Frias, A. Merighi, Capsaicin, nociception and pain. *Molecules* **21**, 797 (2016).

16. C. Grienberger, A. Konnerth, Imaging calcium in neurons. *Neuron* **73**, 862–885 (2012).

17. M. A. Green, M. J. Keevers, Optical properties of intrinsic silicon at 300 K. *Prog. Photovolt Res. Appl.* **3**, 189–192 (1995).

18. H. Dana, Y. Sun, B. Mohar, B.K. Hulse, A.M. Kerlin, J.P. Hasseman, G. Tsegaye, A. Tsang, A. Wong, R. Patel, J.J. Macklin, Y. Chen, A. Konnerth, V. Jayaraman, L.L. Looger, E.R. Schreiter, K. Svoboda, D.S. Kim, High-performance calcium sensors for imaging activity in neuronal populations and microcompartments. *Nat. Methods* **16**, 649–657 (2019).

19. S. Schoch, G. Cibelli,G. Thiel, Neuron-specific gene expression of synapsin I: Major role of a negative regulatory mechanism. *J. Biol. Chem.* **271**, 3317–3323 (1996).

20. A. J. Todd, Neuronal circuitry for pain processing in the dorsal horn Europe PMC Funders Group. *Nat. Rev. Neurosci.* **11**, 823–836 (2010).

21. R. D'Mello, A. H. Dickenson, Spinal cord mechanisms of pain. *Br. J. Anaesth.* **101**, 8–16 (2008).

22. A. Sagner, J. Briscoe, Establishing neuronal diversity in the spinal cord: A time and a place. *Development* **146**, dev182154 (2019).

23. P. J. Osseward II, S. L. Pfaff, Cell type and circuit modules in the spinal cord. *Curr. Opin. Neurobiol.* **56**, 175–184 (2019).

24. H. L. Chong, P. C. Ruben, Interaction between voltage-gated sodium channels and the neurotoxin, tetrodotoxin. *Channels* **2**, 407–412 (2008).

25. Y. Jiang, R. Parameswaran, X. Li, J. L. Carvalho-de-Souza, X. Gao, L. Meng, F. Bezanilla, G. M. G. Shepherd, B. Tian, Nongenetic optical neuromodulation with silicon-based materials. *Nat. Protoc.* **14**, 1339–1376 (2019).

26. J. F. Herrero, J. M. A. Laird, J. A. Lopez-Garcia, Wind-up of spinal cord neurones and pain sensation: Much ado about something? *Prog. Neurobiol.* **61**, 169–203 (2000).

27. D. Budai, A. A. Larson, The involvement of metabotropic glutamate receptors in sensory transmission in dorsal horn of the rat spinal cord. *Neuroscience* **83**, 571–580 (1998).

28. S. G. Khasabov, S. D. Rogers, J. R. Ghilardi, C. M. Peters, P. W. Mantyh, D. A. Simone, Spinal neurons that possess the substance P receptor are required for the development of central sensitization. *J. Neurosci.* **22**, 9086–9098 (2002).

29. J. Coste, D. L. Voisin, L. S. Miraucourt, R. Dallel, P. Luccarini, Dorsal horn NK1-expressing neurons control windup of downstream trigeminal nociceptive neurons. *Pain* **137**, 340–351 (2008).

30. D. Spicarova, V. Nerandzic, J. Palecek, Update on the role of spinal cord TRPV1 receptors in pain modulation. *Physiol. Res.* **63**, S225–S236 (2014).

31. A. Fabbro, A. Villari, J. Laishram, D. Scaini, F. M. Toma, A. Turco, M. Prato, L. Ballerini, Spinal cord explants use carbon nanotube interfaces to enhance neurite outgrowth and to fortify synaptic inputs. *ACS Nano* **6**, 2041–2055 (2012).

32. H.-Y. Zhou, S.-R. Chen, H. Chen, H.-L. Pan, The glutamatergic nature of TRPV1-expressing neurons in the spinal dorsal horn. *J. Neurochem.* **108**, 305–318 (2009).

33. N. P. Pampaloni, M. Lottner, M. Giugliano, A. Matruglio, F. D'Amico, M. Prato, J. A. Garrido, L. Ballerini, D. Scaini, Single-layer graphene modulates neuronal communication and augments membrane ion currents. *Nat. Nanotechnol.* **13**, 755–764 (2018).

34. C. Torsney, A. B. MacDermott, Disinhibition opens the gate to pathological pain signaling in superficial neurokinin 1 receptor-expressing neurons in rat spinal cord. *J. Neurosci.* **26**, 1833–1843 (2006).

35. W. Zieglgänsberger, Substance P and pain chronicity. *Cell Tissue Res.* **375**, 227–241 (2019).

36. F. Furlan, G. Taccola, M. Grandolfo, L. Guasti, A. Arcangeli, A. Nistri, L. Ballerini, ERG conductance expression modulates the excitability of ventral horn GABAergic interneurons that control rhythmic oscillations in the developing mouse spinal cord. *J. Neurosci.* **27**, 919–928 (2007).

37. J. Dimidschstein, Q. Chen, R. Tremblay, S. L. Rogers, G.A. Saldi, L. Guo, Q. Xu, R. Liu, C. Lu, J. Chu, J. S. Grimley, A.R. Krostag, A. Kaykas, M. C. Avery, M. S. Rashid, M. Baek, A. L. Jacob, G. B. Smith, D. E. Wilson, G. Kosche, I. Kruglikov, T. Rusielewicz, V. C. Kotak, T. M. Mowery, S. A. Anderson, E. M. Callaway, J. S. Dasen, D. Fitzpatrick, V. Fossati, M. A. Long, S. Noggle, J. H. Reynolds, D. H. Sanes, B. Rudy, G. Feng, G. Fishell, A viral strategy for targeting and manipulating interneurons across vertebrate species. *Nat. Neurosci.* **19**, 1743–1749 (2016).

38. D. Avossa, M. D. Rosato-Siri, F. Mazzarol, L. Ballerini, Spinal circuits formation: A study of developmentally regulated markers in organotypic cultures of embryonic mouse spinal cord. *Neuroscience* **122**, 391–405 (2003).

39. O. Kiehn, Decoding the organization of spinal circuits that control locomotion. *Nat. Rev. Neurosci.* **17**, 224–238 (2016).

40. L. Ballerini, M. Galante, M. Grandolfo, A. Nistri, Generation of rhythmic patterns of activity by ventral interneurones in rat organotypic spinal slice culture. *J. Physiol.* **517**, 459–475 (1999).

41. M. Passafaro, V. Piëch, M. Sheng, Subunit-specific temporal and spatial patterns of AMPA receptor exocytosis in hippocampal neurons. *Nat. Neurosci.* **4**, 917–926 (2001).

2. D. E. Clapham, D. Julius, C. Montell, G. Schultz, International union of pharmacology. XLIX. Nomenclature and structure-function relationships of transient receptor potential channels. *Pharmacol. Rev.* **57**, 427–450 (2005).

43. M. J. Caterina, M. A. Schumacher, M. Tominaga, T. A. Rosen, J. D. Levine, D. Julius, The capsaicin receptor: A heat-activated ion channel in the pain pathway. *Nature* **389**, 816–824 (1997).

44. J. Luboeinski, T. Tchumatchenko, Nonlinear response characteristics of neural networks and single neurons undergoing optogenetic excitation. *Netw. Neurosci.* **1**, 852–870 (2020).

45. C. Peirs, R. P. Seal, Neural circuits for pain: Recent advances and current views. *Science* **354**, 578–584 (2016).

46. A. J. Christensen, S. M. Iyer, A. François, S. Vyas, C. Ramakrishnan, S. Vesuna, K. Deisseroth, G. Scherrer, S. L. Delp, In vivo interrogation of spinal mechanosensory circuits. *Cell Rep.* **17**, 1699–1710 (2016).

47. K. Montgomery, S. Iyer, A. Christensen, K. Deisseroth, S. L. Delp, Beyond the brain: Optogenetic control in the spinal cord and peripheral nervous system. *Sci. Transl. Med.* **8**, 337rv5 (2016).

48. C. McClure, K. L. H. Cole, P. Wulff, M. Klugmann, A. J. Murray, Production and titering of recombinant adeno-associated viral vectors. *J. Vis. Exp.* e3348 (2011).

49. J. Schindelin, I. Arganda-Carreras, E. Frise, V. Kaynig, M. Longair, T. Pietzsch, S. Preibisch, C. Rueden, S. Saalfeld, B. Schmid, J.-Y. Tinevez, D. J. White, V. Hartenstein, K. Eliceiri, P. Tomancak, A. Cardona, Fiji—An open platform for biological image analysis. *Nat. Methods* **9**, 676–682 (2009).

50. M. A. Green, Self-consistent optical parameters of intrinsic silicon at 300K including temperature coefficients. *Sol. Energy Mater. Sol. Cells* **92**, 1305–1310 (2008).